Electronic Supplementary Material

Making Ultrafine and Highly-Dispersive Multimetallic Nanoparticles in Three-Dimensional Graphene with Supercritical Fluid as Excellent Electrocatalyst for Oxygen Reduction Reaction

Yazhou Zhou, [*,†] *Clive H Yen,* [‡] *Xiaonong Cheng,* [†] *Chien M. Wai,* [‡] *Juan Yang,* [*,†]

[†]School of Materials Science and Engineering, Jiangsu University, Zhenjiang 212013, People's Republic of China

[‡]Department of Chemistry, University of Idaho, Moscow, Idaho 83844-2343, United States

[*]E-mail: zhouyazhou60@gmail.com; yangjuan6347@mail.ujs.edu.cn

KEYWORDS: 3D graphene; ultrafine size; highly-dispersive; supercritical fluid; electrocatalyst; oxygen reduction reaction

Synthesis of 3D HSG

3D HSG was provided by Dr. Hu Y.H (Michigan Technological University, USA). It was synthesized based on the reaction between lithium oxide (Li_2O) and carbon monoxide (CO). 1.0 mol of Li_2O power (Aldrich) was loaded into a ceramic tube reactor and exposed to CO at pressure of 35 psi. The reactor temperature increased from room temperature to 550 °C at a rate of 10 °C min^{-1} and then kept at 550 °C for a 12 h. The prepared black product was treated with diluted hydrocholoric acid (HCl, 36.5 wt%) and washed with deionized (DI) water for more than 10 times to remove

Li_2O, Li_2CO_3 and impurities. Finally, the product was dried overnight at 80 °C to get 3D HSG powder.

The electrochemical surface area (ECSA) of each catalyst was determined using the mean integral charge of the hydrogen adsorption/desorption areas in CV [1]:

$$ECSA = \frac{Q_H}{0.21 \times [Pt]} \quad (1)$$

Where Q_H (mC) is the charge due to the hydrogen adsorption/desorption in the hydrogen region (0.05-0.3 V) of the CVs, 0.21 mC cm^{-2} is the electrical charge associated with monolayer adsorption of hydrogen on Pt, and [Pt] is the loading of Pt on the working electrode.

The kinetic current was calculated from the polarization curve using the well-known mass-transport correction according to the Levich-Koutecky equation [2]:

$$1/i = 1/i_k + 1/i_d \quad (2)$$

Where i is the experimentally obtained current, i_k refers to the mass-transport free kinetic current, and i_d the measured diffusion-limited current. The mass activity of the catalysts can be determined via calculation of i_k and normalization to the Pt-loading [3]. From the same experimental data, one can also calculate the specific activity of different catalysts via determination of i_k and normalization with the ECSA.

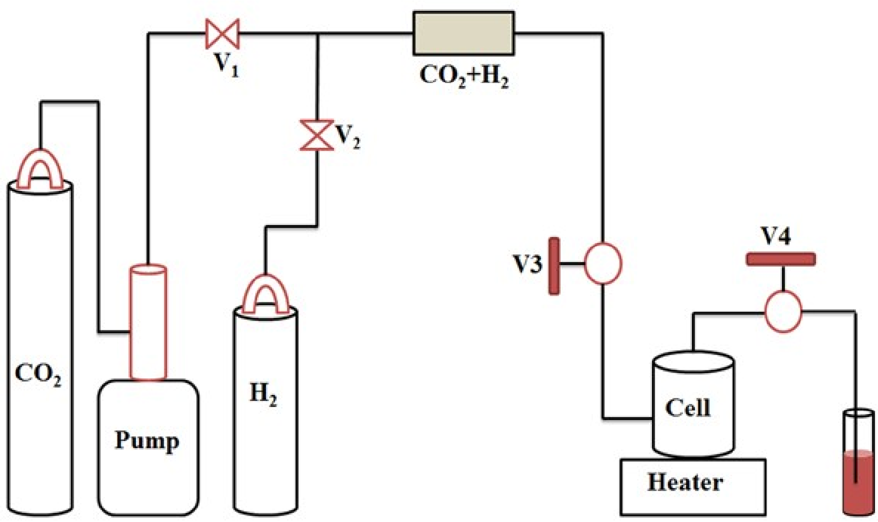

Figure S1. Schematic drawing of the experimental apparatus [23].

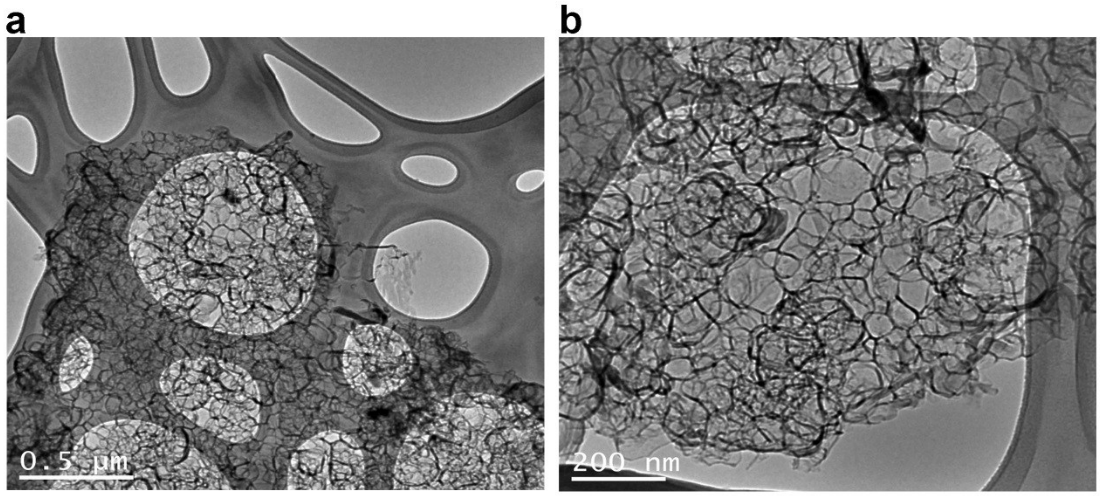

Figure S2. TEM images of 3D honeycomb-structured graphene.

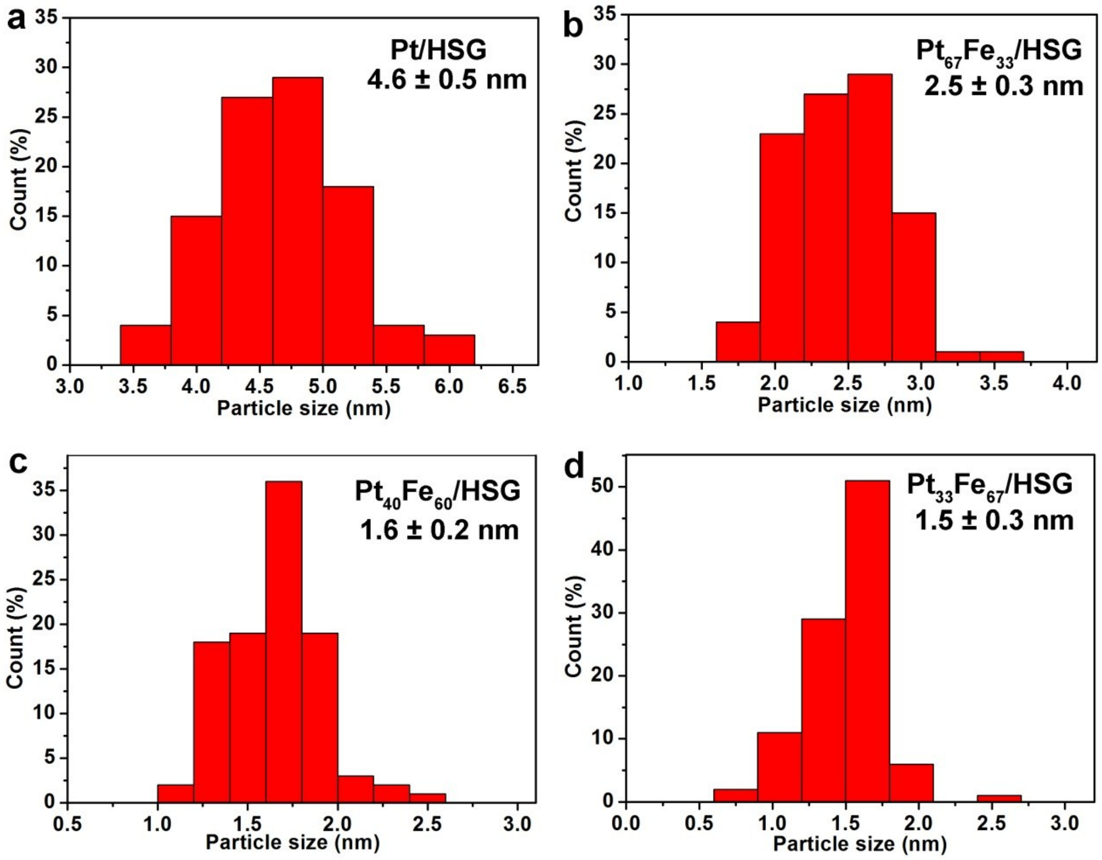

Figure S3. Particle size distributions for Pt/HSG, $Pt_{67}Fe_{33}$/HSG, $Pt_{40}Fe_{60}$/HSG and $Pt_{33}Fe_{67}$/HSG.

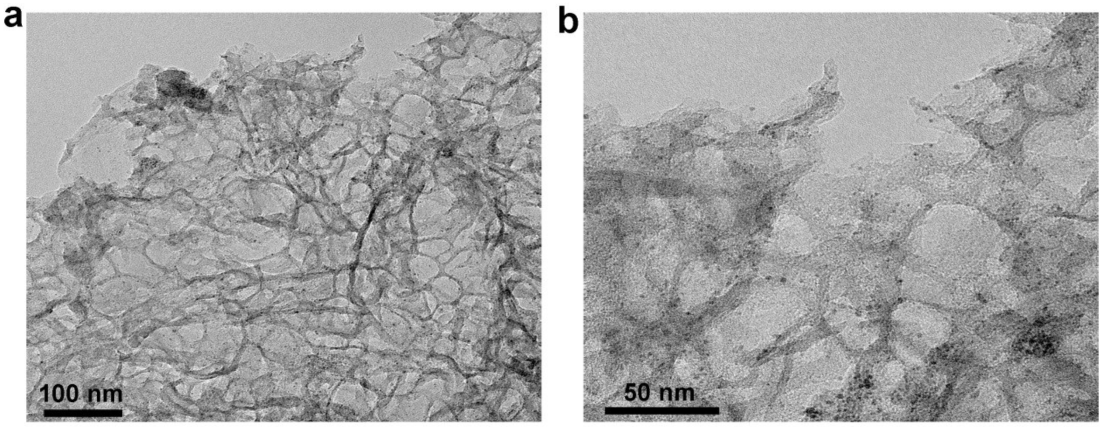

Figure S4. TEM images of $Pt_{40}Fe_{60}$/HSG-1 with low Pt-loading of 5.8 wt%.

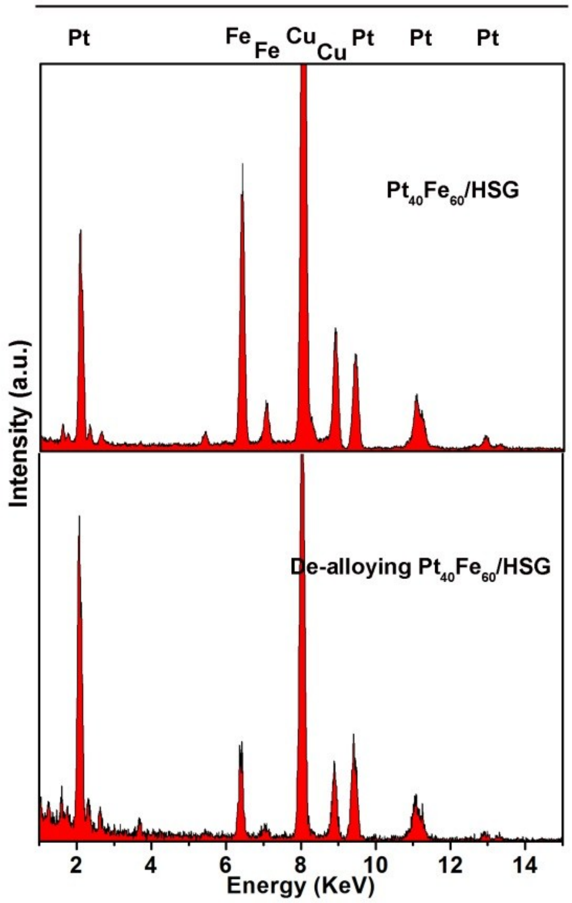

Figure S5. EDX spectra revealing the composition evolving from $Pt_{40}Fe_{60}$/HSG to de-alloying $Pt_{40}Fe_{60}$/HSG (the peaks for Cu come from the TEM grid).

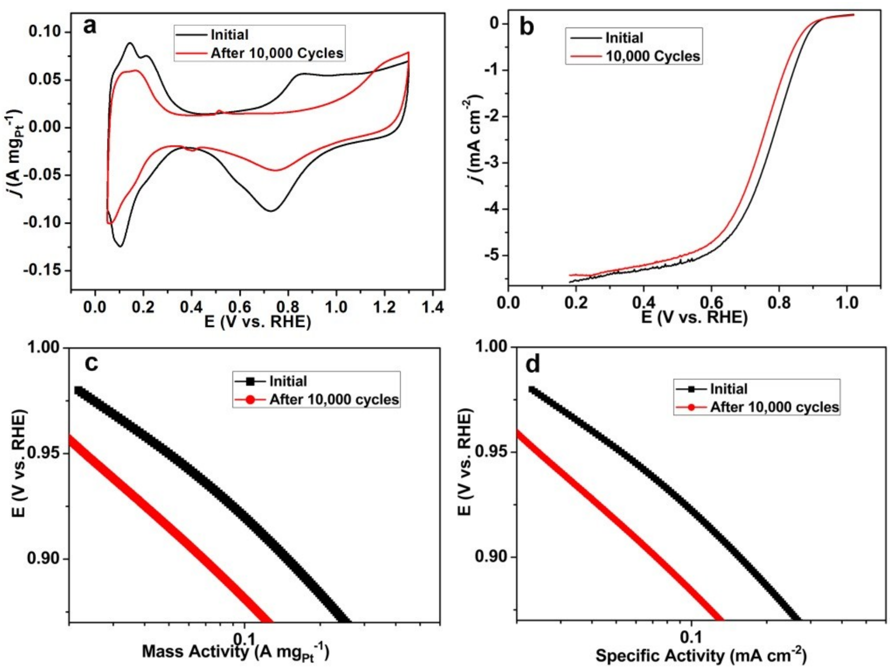

Figure S6. Electrochemical durability of commercial Pt/C catalysts. (a) CVs and (b) ORR polarization curves of commercial Pt/C before and after 10,000 potential cycles between 0.6 and 1.0 with a sweep rate of 200 mV s^{-1}. (c) Mass activity and (d) specific activity of commercial Pt/C catalysts before and after cycles.

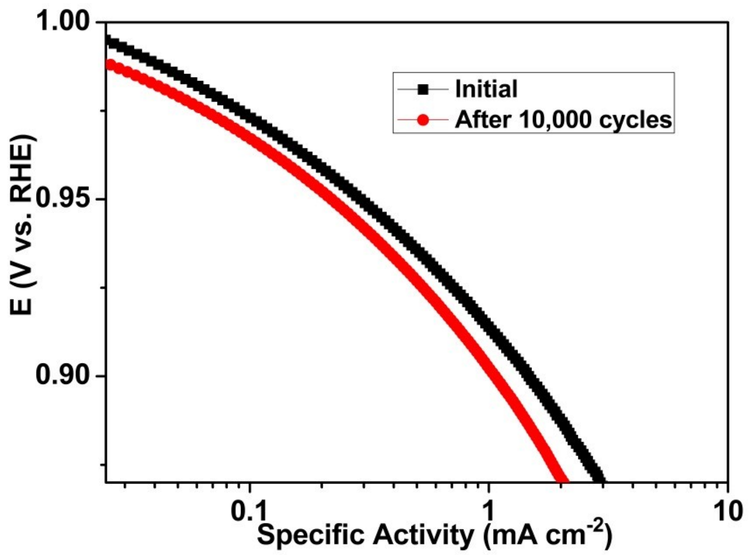

Figure S7. The specific activity of $Pt_{40}Fe_{60}$/HSG catalyst before and after 10,000 cycles.

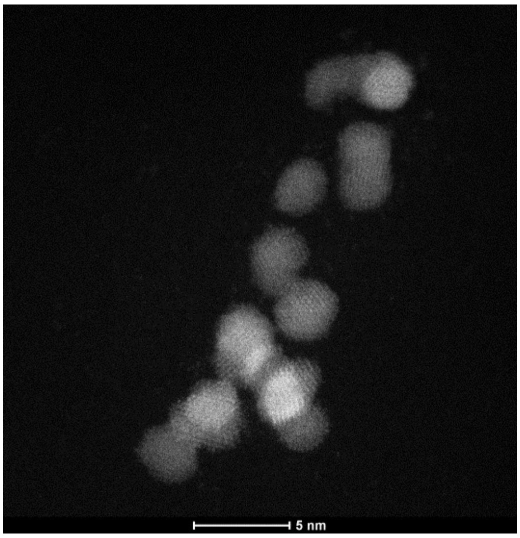

Figure S8. HAADF-STEM image of $Pt_{40}Fe_{60}$/HSG catalyst after 10,000 cycles.

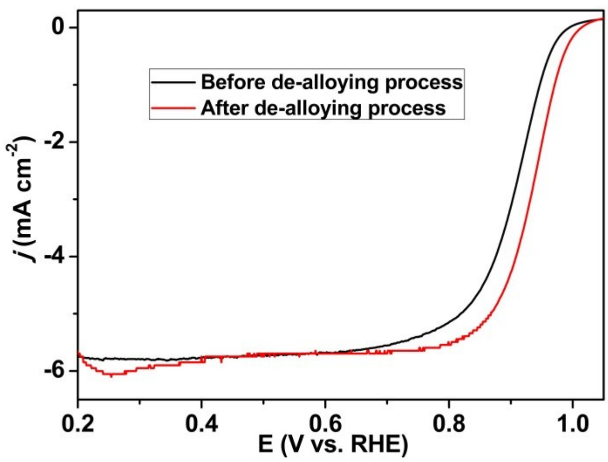

Fig. S9. The ORR polarization curves of $Pt_{40}Fe_{60}$/HSG catalyst before and after de-alloying process.

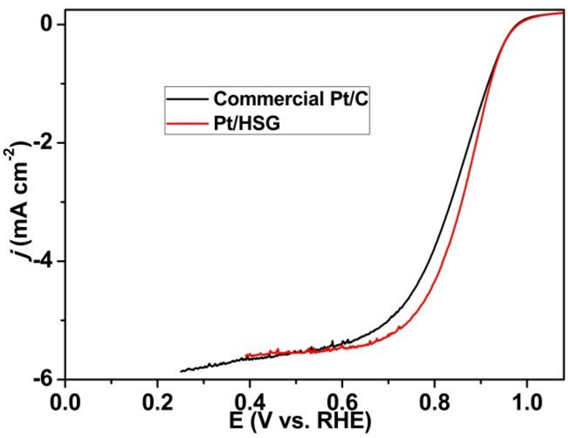

Fig. S10. The ORR polarization curves of Pt/HSG and commercial Pt/C catalysts.

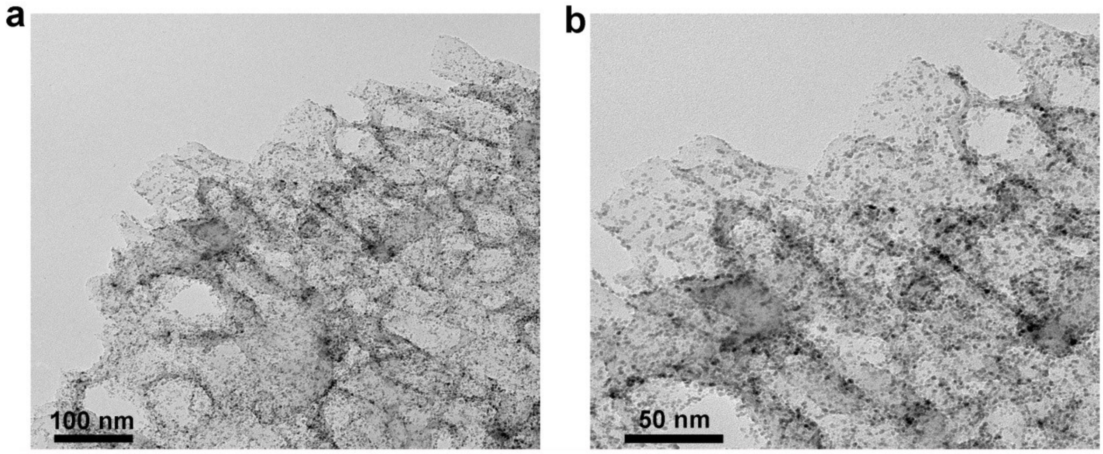

Figure S11. TEM images of $Pt_{55}Ni_{45}$ NPs supported by HSG.

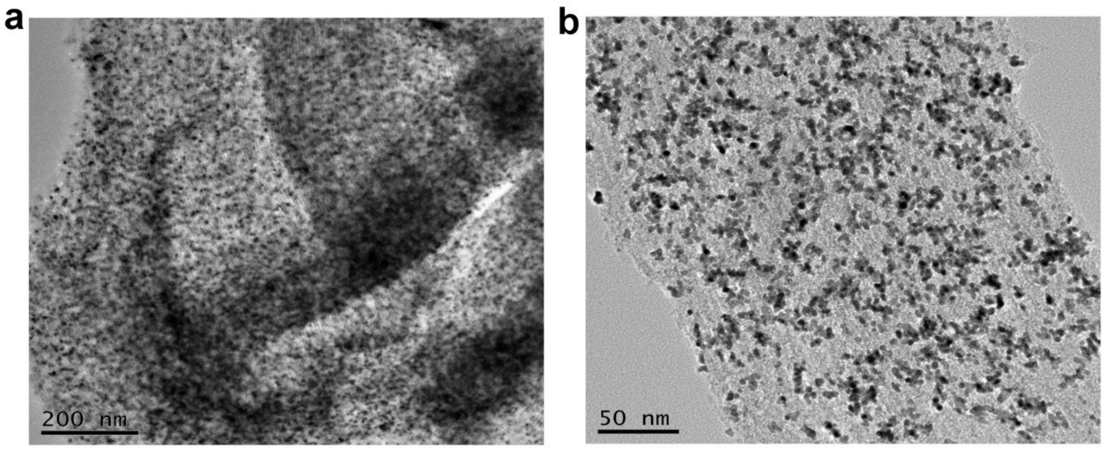

Figure S12. TEM images of Pt NPs supported by mesoporous carbon.

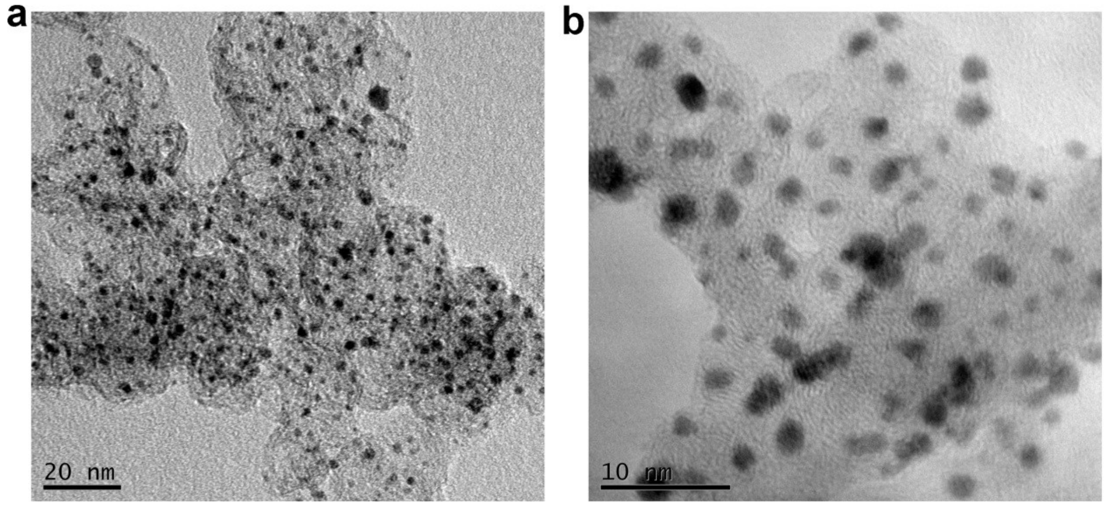

Figure S13. TEM images of $Pt_{40}Fe_{60}$ NPs supported by carbon black with high surface area.

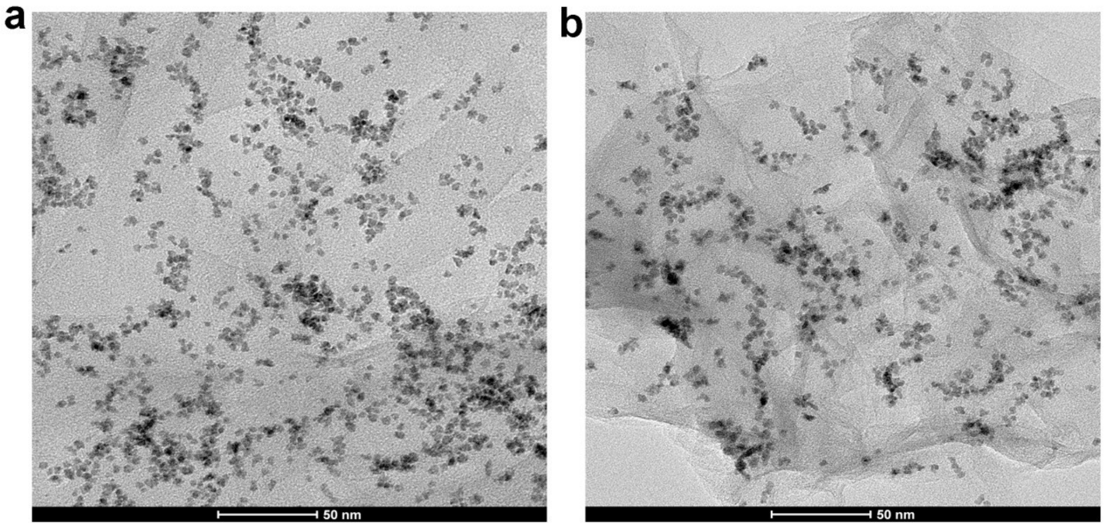

Figure S14. TEM images of $Pt_{40}Fe_{40}Ir_{20}$ NPs supported by 2D graphene.

Table S1. Summary of electrochemical performance results.

Catalyst	ECSA ($m^2\ g_{Pt}^{-1}$)	Mass activity (at 0.9 V/A mg_{Pt}^{-1})	Specific activity (at 0.9 V/mA cm^{-2})
$Pt_{67}Fe_{33}$/HSG	85	0.60	0.71
$Pt_{40}Fe_{60}$/HSG	110	1.70	1.55
$Pt_{33}Fe_{67}$/HSG	82	0.90	1.09
Pt/C	95	0.12	0.13

Table S2. Comparison of durability of $Pt_{40}Fe_{60}$/HSG catalyst with that of commercial Pt/C.

Catalyst	ECSA ($m^2\ g_{Pt}^{-1}$)		Mass activity (at 0.9 V/A mg_{Pt}^{-1})		Specific activity (at 0.9 V/mA cm^{-2})	
	Initial	ADT	Initial	ADT	Initial	ADT
$Pt_{40}Fe_{60}$/HSG	110	100	1.67	1.20	1.55	1.08
Commercial Pt/C	95	42	0.13	0.07	0.14	0.07

References

[1] Guo, S.; Zhang, S.; Su, D.; Sun, S. Seed-Mediated Synthesis of Core/Shell FePtM/FePt (M = Pd, Au) Nanowires and Their Electrocatalysis for Oxygen Reduction Reaction. *J. Am. Chem. Soc.* **2013**, *135*, 13879-13884.

[2] Schmidt, T. J; Gasteiger, H. A. Rotating thin-film method for supported catalysts, in: W. Vielstich, H. Gasteiger, A. Lamm (Eds.), Handbook of Fuel Cells-Fundamentals, Technology and Applications, vol. 2, Wiley, 2003, p. 316 (Chapter 22).

[3] Gasteiger, H. A.; Gu, W.; Makharia, R.; Mathias, M. F.; Sompalli, B. Beginning-of-life MEA performance: efficiency loss contributions, in: W. Vielstich, A. Lamm, H.A. Gasteiger (Eds.), Handbook of Fuel Cells-Fundamentals, Technology and Applications, vol. 3, Wiley, Chichester, UK, 2003, p. 593 (Chapter 46).